Journal of Al-Azhar University Engineering Sector

Vol. 17, No. 65, October 2022,1362-1375

RECYCLING OF WASTE OYSTER SHELLS AS A REINFORCEMENT MATERIALS FOR AA7075 ALLOY

H. A. Fattah [1,2]

[1]Mining and Pet. Dept, Faculty of Engineering, Al-Azhar University, Nasr City, Egypt

[2]Alexandria Higher Institute of Engineering and Technology (AIET), Alexandria,21311, Egypt

*Corresponding: hasanfattahy2008@yahoo.com

Received: 1 September 2022 Accepted: 22 September 2022

ABSTRACT

In the current research, oyster shells have been recycled by reinforcing with aluminum alloy AA7075 using the stir casting method. The oyster shells (OS) were washed and milled via high energy ball mill. The produced castings were fabricated with various content of the OS particles as (0-15 Wt.%). The effect of oyster shell particles (OS) on the microstructures, mechanical properties and corrosion behavior of AA7075/OS composites has been studied. The microstructure results revealed a uniform distribution of oyster shell particles within AA7075 matrix. Compression, brinell hardness, and impact tests of the sample were carried out to identify the mechanical properties of the composite. The hardness was increased from 37%, 61% and 88.7% for AA7075 reinforced with 5, 10 and 15% OS composite compared with unrienforced AA7075. On the other hand, the ultimate compressive strength was improved from 10.7%, 19.8% and 25.9% for AA7075 reinforced with 5, 10 and 15% OS composite compared with unreinforced AA7075. The corrosion rate and weight loss method were carried out by immersing the specimens in 0.1M NaOH and 0.1M H_2SO_4 solutions. Results revealed that the rate of corrosion and mass loss were decreased with an increase of mass fraction up to 15%.

Keywords: Stir Casting, Oyster shell, Composites, Mechanical properties, Corrosion rate.

إعادة تدوير نفايات المحار وإستخدامها كمواد مقوية لسبيكة ٧٠٧٥

حسن عبد الفتاح عبد الفتاح متولي

[١] قسم هندسة التعدين والبترول ، جامعة الازهر، القاهرة، مصر

[٢] معهد اسكندرية العالي للهندسة والتكنولوجيا، الأسكندرية، مصر

* البريد الإلكتروني للمؤلف الرئيسي: hasanfattahy2008@yahoo.com

الملخص

قشور المحار (OS) هي واحدة من النفايات التي تنتج بكميات كبيرة كل يوم. وفي البحث الحالي ، تم إعادة تدوير أصداف المحار من خلال استخدامها كواد مقوية لسبيكة الألومنيوم AA7075 باستخدام طريقة الصب بالتحريك. في البداية تم غسل وطحن قشور المحار (OS) في طاحونة كروية عالية الطاقة. تم تشكيل المصبوبات المنتجة وتصنيع العينات بمحتوى مختلف من حبيبات OS بنسبة (٠-١٥٪ بالوزن). تمت دراسة تأثير جزيئات قشرة المحار (OS) على التركيب الداخلي والخصائص الميكانيكية وسلوك التآكل لمركبات AA7075 / OS. أوضحت النتائج أن توزيع منتظم لجسيمات حبيبات المحار داخل مصفوفة AA7075. تم إجراء ضغط ثم اختبار الصلابة بطريقة برينيل (صلابة برينل) واختبار الصدم للعينات لتحديد الخواص الميكانيكية للمركب. أظهرت النتائج زيادة الصلابة من ٣٧٪ و ٦١٪ و ٨٨,٧٪ بالنسبة للـ AA7075 المقواة بمركب ٥ و ١٠ و ١٥٪ OS مقارنة مع العينات غير المقواه AA7075. بالإضافة إلى ذلك ، تم تحسين مقاومة الخضوع من ٢٢,٧٪ و ٣٨,٦٪ و ٥٤,٤٪ لـ AA7075 المقواة بمركب ٥ و ١٠ و ١٥٪ OS مقارنة مع AA7075 غير المقوى. من ناحية أخرى ، تم تحسين مقاومة الانضغاط القصوى من ١٠,٧٪ و ١٩,٨٪ و ٢٥,٩٪ لـ AA7075 معززة بمركب ٥ و ١٠ و ١٥٪ OS مقارنة مع AA7075 غير المقوى. تم إجراء اختبار لدراسة سلوك التآكل للعينات وذلك باستخدام طريقة فقدان الوزن عن طريق غمر العينات في محلول ٠,١ مولار هيدروكسيد الصوديوم و ٠,١ مولار H_2SO4 لمدة ٣٠ يومًا ، بفاصل ٥ أيام. أوضحت النتائج أن معدل التآكل وفقدان الكتلة انخفض مع زيادة نسبة قشور المحارفي العينات حتى ١٥٪. بالإضافة إلى ذلك ، كان معدل التآكل وفقدان الكتلة أقل في محلول هيدروكسيد الصوديوم ٠,١ مولار مقارنة بمحلول ٠,١ مولار H_2SO4.

الكلمات المفتاحية : صب التحريك ، قشرة المحار ، المواد المركبة ، الخواص الميكانيكية ، معدل التآكل.

1. INTRODUCTION

In current period, there has been an increase in needs to light-weight, cost-effective engineering materials with higher strength, particularly in different engineering applications to improve performance [1]. Interestingly, aluminum and its alloys with matching characteristics of light weight, low cost, good thermal and electrical properties desirable in various engineering applications had stimulated research interest. However, as illustrated in earlier articles, aluminum composite materials are becoming more popular in engineering applications due to their lighter weight and enhanced mechanical and thermal characteristics when compared to conventional Al alloys. Due to their owing characteristics such as high specific strength and young's modulus, cheap cost, and strong wear resistance, aluminum metal matrix composites (AMMCs) have a distinct place in the automotive and aerospace industries [2,3]. AMMCs are fabricated materials produced by introducing nonmetallic additions to Al metal or Al alloys to adapt characteristics including strength, hardness, stiffness, electrical and thermal conductivity, and other mechanical characteristics [4]. Previous articles showed many factors influencing the material's properties, including the type of reinforcement, manufacturing method, volume or mass fraction, particle size, shape, and distribution of reinforcement within the matrix [5]. Carbides, oxides, and carbides such as SiC, Al2O3, TiB, TiC, etc are commonly used as reinforcements to strengthen aluminum and its alloys [6]. The cost of reinforcement has an impact on the applications of AMMCs; thus it has become vital to find low-cost reinforcing materials to improve their uses. According to its low cost and high mechanical properties, natural waste has become a more popular reinforcement material in AMMCs production in recent years. On the other hand, using natural waste as a reinforcement material is a good method to get rid of large quantities of waste that have no feasible economic benefit. Oyster shells (OS) are one of the most calcium-rich natural wastes, with around 95% $CaCO_3$, followed by Cu, Ni, Co, and Fe oxide [7], and the least expensive [8]. MMCs have been made using different methods, including liquid metallurgy [9], powder metallurgy [10], in situ synthesis [11], and spray forming [12]. The liquid metallurgy route includes the stir casting method. This method has a variety of advantages, including ease of use, low production costs, flexibility, high amount production, high metal output, no harm to reinforcement, no shape or size constraints, etc [13,14]. Fabrication, and characterization of AA7075 composites using artificial additions for example TiO_2, Al_2O_3, SiC, B4C, etc has been studied by a number of researchers [15-19]. Most researchers are now focusing on using natural sources of

reinforcement for example, Singla and Mediratta [20] evaluated the characteristics of as-cast AA7075 reinforced with fly ash, the composite was fabricated via stir casting technique and Mg was introduced to improve the wettability of reinforcement in AA7075 molten. Dwivedi et al. [21] used electromagnetic stir casting and hot extrusion to manufacture hybrid AA2014/SiC/eggshells composites. The results showed that a sample containing 2.5 wt% SiC and 7.5 wt% CES has the highest mechanical characteristics and highest density. Gupta and Singh [22] investigated the effect of various forms of natural waste on the microstructure and mechanical properties of AA7075 composites, such as rice husk ash, poultry waste, and eggshells. The results showed that the AA7075/5 wt. % rice husk ash composite had the maximum hardness value, improving by 24.47 % over pure matrix. Also, when the AA7075 was reinforced with 3.75 and 1.25 wt. % rice ash and ES (eggshell), respectively, the maximum tensile and compressive strength was obtained. According to prior reports, only a few studies have used natural waste as a reinforcement, particularly oyster shell, to produce AA7075-Oyster shell (OS) composites.

In present study, an aluminum alloy 7075 (AA7075) composite reinforced with oyster shells (OS) particles is fabricated using a stir casting method. The microstructure, mechanical characteristics and immersion corrosion are investigated and estimated, and the results are compared with pure AA7075 matrix.

2. MATERIALS AND METHODS

2.1. Materials

Oyster shells (OS) were collected from a Red Sea beach in Egypt, rinsed with water, dried in the oven to eliminate excess moisture, and then broken into small pieces by a jaw crusher (Figure 1a). Then the small oyster shell pieces were milled to powder via high energy ball mill at 300 revolutions per minute (rpm) as shown in Fig 1 b. OS powder was calcinated at high temperatures (1000 °C) for 1 hour to remove low valent oxides and release a massive proportion of volatiles (Fig 1c). After that, the powder was passed over sieves of various sizes to obtain particles with a consistent size distribution. Table.1[23] shows the chemical constitution of oyster shell.

Fig 1: (a) Oyster shell collected from red sea (b) oyster shell powder after crushing in ball mill (c) Oyster shell powder after calcination for 1000 ℃ for a period of 1 hour

Table.1 Chemical Composition of Oyster shell (by Wt%) [23].

Constituent	SiO_2	Fe_2O_3	CaO	MnO_3	MgO	Na_2O	SO_3	TiO_2	P_2O_5	Al_2O_3
% wt	26.26	4.82	55.53	0.05	0.4	0.25	0.18	0.2	0.05	8.79

The matrix in current research is aluminum alloy 7075 (AA7075), which displays good casting characteristics and widely used alloy. In comparison to other aluminum alloys, alloy 7075 has unique

properties such as high ductility, high strength, toughness, and excellent fatigue resistance, however it is less corrosion resistant. The chemical composition and mechanical properties of AA7075 alloy used in the present work are shown in table 2 and 3[22].

Table 2 Chemical Composition of AA7075

Elements	Si	Fe	Cu	Mn	Mg	Cr	Zn	Ti	Al
% wt	0.4	0.5	2.0	0.3	2.9	0.28	6.1	0.2	Balance

Table 3 Mechanical properties of AA7075

UTS	225-570 MPa
Shear stress	150-350 MPa
Brinell hardness Number	65-70 MPa
Elasticity	72000 MPa
Poisson Ratio	0.33

2.2. Preparation of Composite

Electric furnace was used to melt AA7075 with Oyster shell (OS) reinforcement. The melting was carried out in a ceramics crucible placed inside the electric furnace, which is then heated to above melting temperature 750°C. The calcined oyster shells (OS) with different mass fractions from (0 to 15wt %) were added to molten metal. The melt temperature was kept at 750°C while adding OS reinforcement. Previous to this, magnesium particles (2%) was introduced to the liquid metal to improve wettability of the metal by increasing its surface energy, decreasing the surface tension and reducing the AA7075-OS interface energy [24]. The mixture was continuously stirred at 300 rpm. To ensure regular distribution of oyster shell particles within the molten, both AA7075 alloy and OS particles were kept in the furnace for 5 minutes and continuously stirred. The mixture was then poured into metal moulds and finally dried, giving composites.

2.3. Density determination

ASTM B328 procedures were used to determine the density and relative density of AA7075/OS composites. An electronic balance was used to weigh samples in air, then dipped and weighed in distilled H_2O. The relative density of the composites was calculated using a following equation**:**

$$\text{Relative density\%} = (W_{\text{in H2O}} / W_{\text{in air}}) \times 100 \quad (1)$$

where $\mathbf{W_{in\ H2O}}$ characterizes the weight of specimen in distilled H_2O), $\mathbf{W_{in\ air}}$ refers to the weight of specimen in air. Also, the porosity % was obtained via the following rule:

$$\text{Porosity \%} = (1- (\rho_{\text{experimental}} / \rho_{\text{theoretical}})) \times 100 \quad (2)$$

where **Porosity %** is the percentage porosity of the composites, **($\rho_{\text{experimental}}$)** is the experimental density, while (**($\rho_{\text{theoretical}}$)**) is the theoretical density.

2.4. Microstructural evaluation

SEM and EDS (JEOL (model JSM). No – (6330F) microscope at a voltage of 20 keV) were used to examine the microstructure of an AA7075 alloy reinforced with oyster shells (OS) particles. All samples were prepared by grinding with 350, 600,1000 and 1200 grid SiC paper, respectively. Subsequently, the samples were polished with alumina and washed, and Keller solution was used to disclose their microstructure.

2.5. Hardness Test

The Brinell hardness test according (ASTM E10) was carried out on the unreinforced AA7075 and AA7075/OS composites to evaluate the mechanical behavior. Brinell hardness (BHN) was measured in the current research using a **Mettoya hardness tester** with a **5000 N** load and a 10 mm diameter steel ball indenter. The hardness values have also been checked for reproducibility with 3 specimens under the same conditions. The results cited are the average values from such multiple tests. Calculations using the following formula give the B.H.N (Brinell Hardness Number) [25]:

$$\mathbf{B.H.N} = \frac{\mathbf{2P}}{\mathbf{\pi D(D-\sqrt{D^2-d^2})}} \qquad \mathbf{(3)}$$

Where P = Force applied (kg), D = Diameter of indenter (mm) and d = Diameter of indentation (mm)**.**

2.6. Compression Test

Compression testing was performed on 5 mm radius and 10 mm height. The test was achieved at an initial strain rate of 0.5mm/min, using a testing machine (**com-ten with program software 2.1.25**). Compression specimens were cut from the unreinforced AA7075 and AA7075/OS composites using a wire cutting machine. The compression test results are based on an average of three independent test values for each specimen**.** The specimen is located between two flat dies and the die surfaces are lubricated. The maximum failure load was measured by compressing the sample between two flat platens.

2.7. Impact Test.

The impact test samples were prepared according to the ASTM-E23 standard using pendulum type testing machine (Gunt HAMBURG wp 400) as shown in Fig 2 a. The impact specimen has dimensions 55 mm x 10 mm x5 mm with a Charpy V notch as shown in Fig 2b. The test was performed at 25 °C and the impact energy values were read directly for three samples in each case to get the average value.

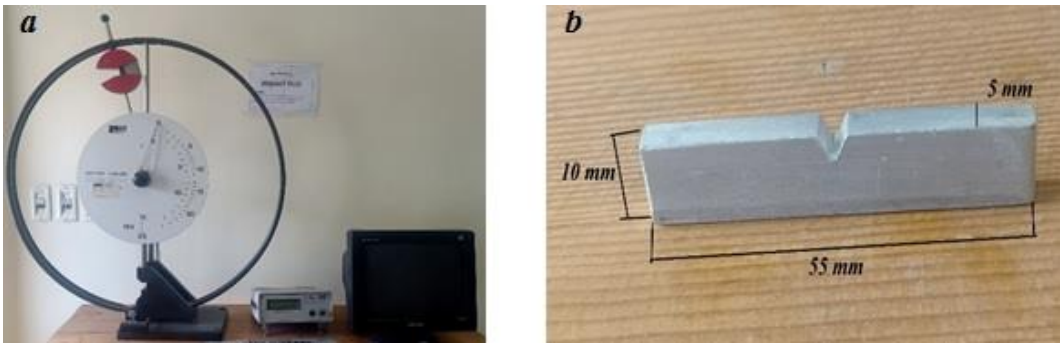

Fig 2. photograph of (a) testing machine (Gunt HAMBURG wp 400) (b) Charpy impact specimen

2.8. Immersion Corrosion Test

The Immersion corrosion tests were performed for both as cast AA7075 and AA7075/OS composites containing a varied mass fraction of OS particles in two different corrosion environments. The test

specimens were cut to a diameter of 20 mm and a thickness of 10 mm, after which the samples' surfaces were polished with abrasive papers of various grit sizes. Immersion corrosion tests on 0.1M NaOH and 0.1M H_2SO4 solutions were conducted every 5 days for 30 days. Further, the samples were rinsed with a standard solution, washed with distilled H_2O, and then immersed in 0.1M NaOH and 0.1M H_2SO4 solutions. An electronic digital weighing balance (a four-decimal digit electronic weighing balance) was used to estimate the loss in the sample mass throughout the immersion corrosion test. According to ASTM G31 standards, weight loss for every specimen was calculated. Also, the corrosion rate was estimated using the below equation [26]:

$$\text{Corrosion Rate (mpy)} = \frac{534\ \text{w}}{\rho \text{At}} \tag{4}$$

Where, $\boldsymbol{\rho}$ is the sample density in (g/cm^3); $\boldsymbol{A}$ is the area of the sample (inch^2), and $\boldsymbol{t}$ refer to the contact time in hr and **w** represents the weight loss in (mg).

3. RESULTS AND DISCUSSION

3.1. Density measurement

The density measurements of the as cast AA7075 and AA7075/OS composites containing different mass fraction of OS particles were evaluated. Experimental and theoretical densities were calculated by Archimedes principle and Mixture rule, respectively (see Fig 3). As shown in Fig 3, the experimental and theoretical density of unreinforced AA7075 were 2.77 and 2.81 g/cm3, respectively. With an increase in OS mass fraction, the theoretical density of composites starts to drop. Moreover, the computed density for as cast AA7075 and AA7075/OS composites was reported to be lower than theoretical values. The overall experimental density of AA7075/OS composites reduced with wt.% additions of OS reinforcement e.g., the density of the composites declined from 2.77 g/cm^3 at 0 wt.% to 2.33 g/cm^3 at 15 wt.% of oyster shell.

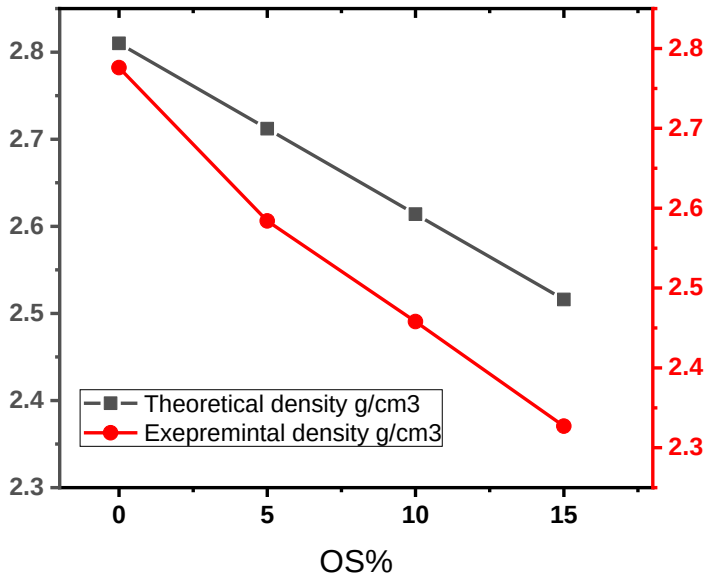

Fig 3. Experimental and theoretical density of AA7075 and composites with different mass fraction of OS.

The relative density for of as cast AA7075 was observed to be greatest with compared to that of composites. The maximum density was calculated for as cast of AA7075 and lowest for composite at 15 wt% of oyster shell particles as can be seen in the Fig 4. On the other hand, % porosity was computed by dividing the difference of theoretical and experimental density by theoretical density as shown in equation 2. Here, the porosity of as cast of AA7075 and AA7075 /15% OS composite were 1.2 and 7.5%, respectively. The existence of low ceramics material density in composites, such like oyster shell particles, is The major cause of the decline in relative density and increase in porosity %.

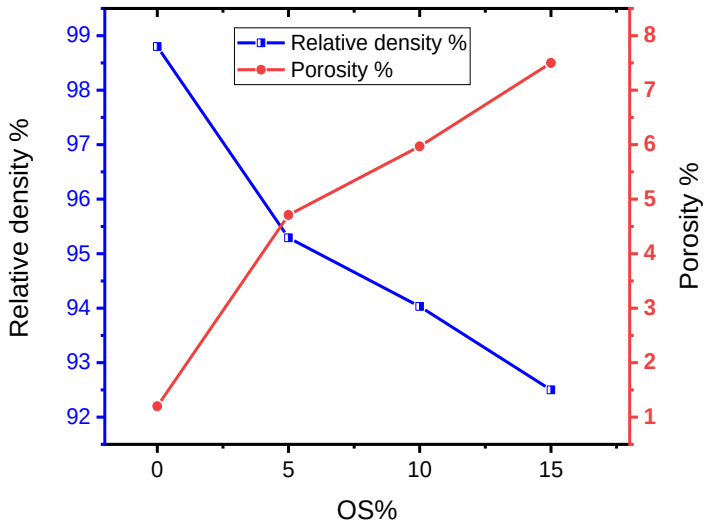

Fig 4. Relative density and porosity percentage of pure AA7075 and composites with different mass fraction of OS.

3.2. Microstructure Evaluation

Fig 5(a- c) shows the SEM and EDS images of pure AA7075 and 15 wt.% OS composites. The presence of OS in the composites is confirmed by these microstructures. The OS particle distribution was rather homogeneous, with little clumping. It was discovered that adding OS particles reduces dendritic lengths because the particles act as favourable nucleation sites for matrix solidification. Fig 5 revealed that, when the OS particle content is increased to 15%, the OS particles move and concentrate at the grain boundaries, establishing a homogeneous network and uniformly dispersed inside the matrix. This behaviour is similar to that seen by Efe et al. [27]. The EDS images revealed that a set of elements are regarded to be the primary components of each of the AA7075 matrix and composites, and the most abundant elements were Mg, Zn and Cu. The copper and zinc element concentrations in the AA7075 matrix and composites were 2.7 and 2.67 wt.%, respectively, according to the EDS results shown in Fig. 5(b and d). Also, EDS analysis shows that the amount of Al in the 15 wt. % OS composites has reduced. The decreases in the Al element according to the addition of OS particles within the AA7075 matrix.

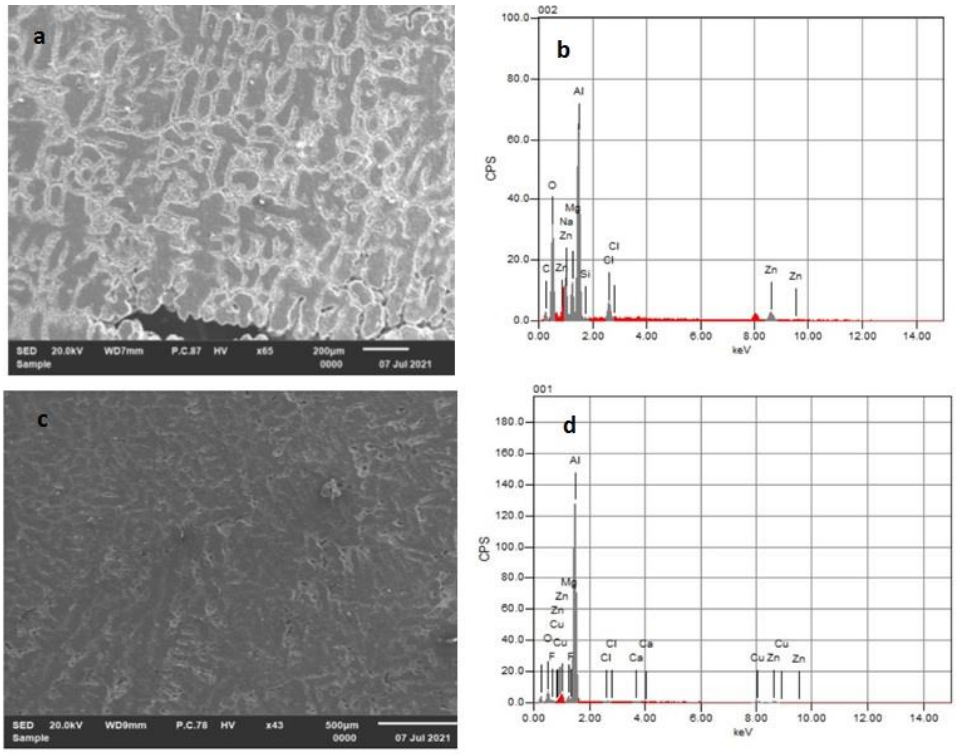

Fig 5(a- c) : SEM and EDS images of pure AA7075 and 15 wt.% OS composites

3.3. Mechanical properties

3.3.1. Hardness Test

Fig 6 displays the influence of oyster shell mass fraction on the hardness of AA7075 composites. The loading of OS reinforcement to the AA7075 matrix lead to improvement in the brinell hardness number (BHN) as distinguished in Fig 6. The hardness is improved as the OS mass fraction increases, reaching 117 BHN for the composite sample with 2015% OS particles.

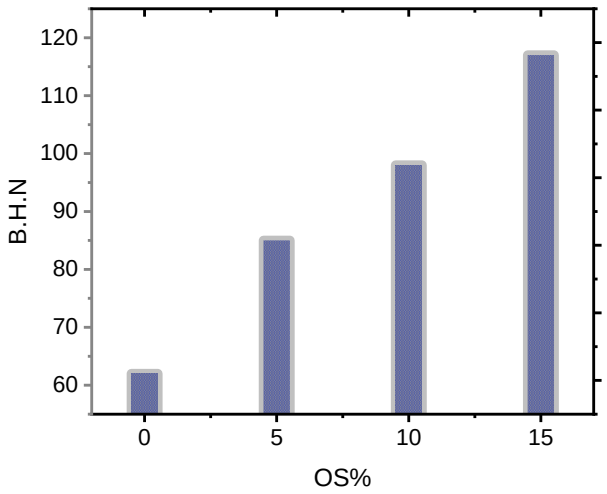

Fig 6. Brinell Hardness Number of unreinforced AA7075 and composites.

The hardness was increased from 37%, 61% and 88.7% for AA7075 reinforced with 5, 10 and 15% OS composite compared with unrienforced AA7075, respectively. The presence of OS particles under the indenter during the hardness test enhances the hardness and gives resistance to plastic deformation. As is common knowledge, the existence of a hard and ceramics reinforcement material such as OS within a soft and ductile matrix like AA7075 can greatly increase the composite's hardness [28, 29].

3.3.2. Compressive Strength

Fig 7, illustrates the effect of waste oyster shell reinforcement mass fraction on the yield and ultimate compressive strength of the unreinforced AA7075 and composites.

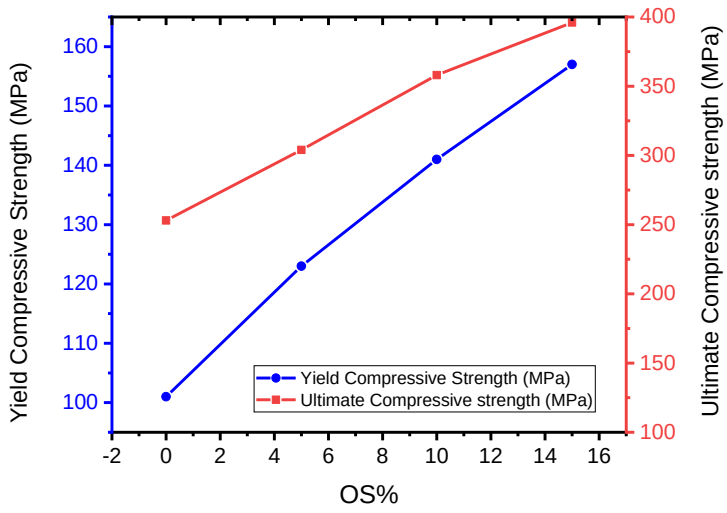

Fig 7. Effect of waste oyster shell particles on yield compressive and ultimate compressive strengths of unreinforced AA7075 and composites.

Both of yield and ultimate compressive strength were calculate by the following equations:

$$\text{Ultimate Compressive strength} = \frac{\text{max load}}{\text{Cross section area A}} \quad (5)$$

$$\text{Yield Compressive strength} = \frac{\text{load at yield point}}{\text{Cross section area A}} \quad (6)$$

Fig 7 shows that the compression strength increases when oyster shell particles of varying mass fractions are added. It is clear that, the incorporation of waste OS reinforcements improved both yield and ultimate compressive strength, as shown in this graph. The yield strength improved from 22.7%, 38.6% and 54.4% for AA7075 reinforced with 5, 10 and 15% OS composite compared with unreinforced AA7075. On the other hand, the ultimate compressive strength improved from 10.7%, 19.8% and 25.9% for AA7075 reinforced with 5, 10 and 15% OS composite compared with unreinforced AA7075. The presence of hard ceramics and oxide phases in oyster shell, particularly CaCO3 and SiO2, may be responsible for this improvement.

3.3.3. Impact Test

In terms of impact energy, all AA7075 composites and unreinforced AA7075 alloys were tested at various mass fractions of waste oyster shell particles, as shown in Fig 8.

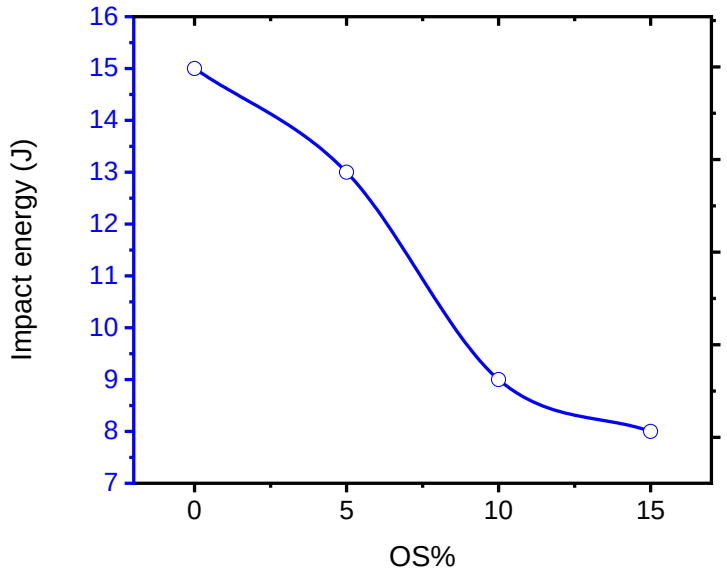

Fig 8. Effect of waste OS particles on the Impact energy (Joule) for AA7075 composites and unreinforced AA7075 alloy.

Fig 8. shows that, all composites have a lower impact strength than unreinforced alloy, indicating that the ductility of the matrix has decreased according to the inclusion of oyster shell reinforcements, which increases the brittleness of AA7075. Other studies have also noticed a significant decline in the addition of filler content [30, 31]. Furthermore, the presence of oyster shell particles within the AA7075 matrix, to the formation of some cavities , holes and pores, which led to a reduction in the impact energy. The results revealed that impact energy declined from 15 (J) for pure AA7075 alloy to 8.1 (J) for AA7075/ 15 % OS.

From the above discussion, the increase in hardness and compressive strength of AA7075 composites, as well as the decrease in impact energy, can be caused by an increase in the mass fraction of ceramics phases of the OS reinforcement within the AA7075 matrix. As seen in the chemical composition of waste oyster shell, the hardness of the OS particles is produced from ceramic phase such as CaCO3 and oxide phase such as SiO2 [23]. Also, the transfer load from AA7075 matrix to OS reinforcement and interface bonding between matrix and OS particles are important to the strengthening of AA7075/OS composites. When the AA7075 matrix composite is loaded, the load was transferred from the AA7075 matrix to the OS reinforcement particle, which increases the composite resistance to plastic deformation due to the variation in thermal mismatch values of the matrix and reinforcement particles.
As mentioned earlier, the presence of oyster shell particles in the AA7075 alloy increases the thermal mismatch between the matrix and OS particles which in turn increases the dislocation density within the AA7075 matrix. A higher dislocation density in the composite results in a higher degree of internal stress, which improves all of the composites mechanical properties [32].

3.4. Corrosion Behavior

3.4.1. Corrosion Behavior in O.1M NaOH Solution

The weight loss and corrosion rate of unreinforced AA7075 and AA7075 reinforced with different mass fractions immersed in the 0.1MNaOH solution are shown in Fig 9 **a** and **b**. The results revealed that the

weight loss of both the pure AA7075 alloy and the AA7075 reinforced by different mass fractions of OS after 30 days in the 0.1M NaOH solution was less than 5 mg.

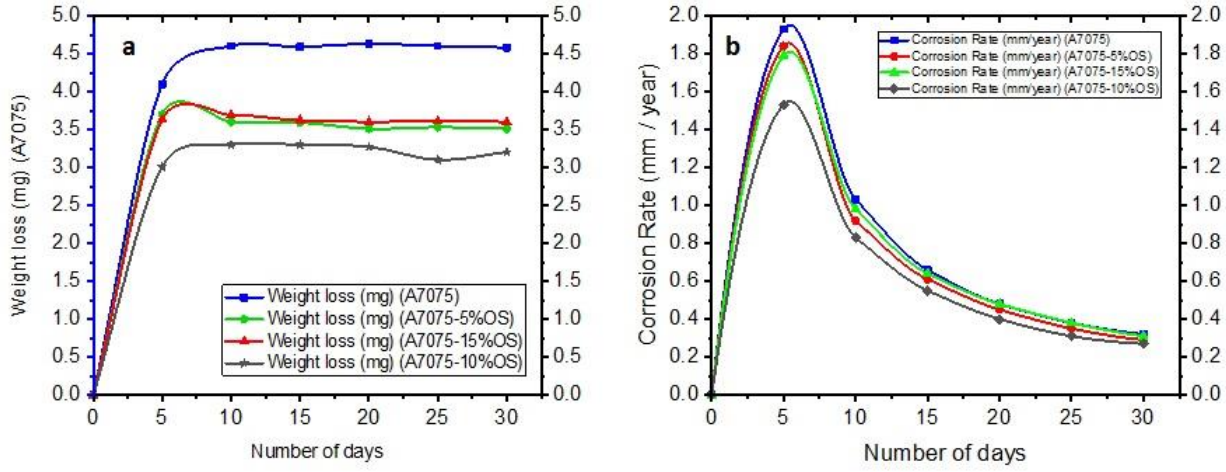

Fig 9 (a, b). Mass loss and corrosion rate of pure AA7075 and composites immersed in 0.1MNaOH solution.

Weight loss was also observed to be insignificant between 15 and 30 days. On the other hand, the corrosion rate of both the pure AA7075 matrix and the AA7075 strengthened by different mass fractions of OS after 30 days in the 0.1M NaOH solution was less than 2 mm / year. In addition, figure 9 **b** shows that the corrosion rate for all the samples was only significant during the first 5 days of immersion in 0.1MNaOH solution, after which it dropped significantly. Finally, it can be seen in fig 9 **a** and **b** that the AA7075 reinforced with 15% OS had a higher corrosion resistance than the other samples.

3.4.2. Corrosion Behavior in 0.1M H_2SO_4 Solution

The weight loss and corrosion rate of unreinforced AA7075 and AA7075 reinforced with different mass fractions immersed in the **0.1M H_2SO_4** solution are shown in Figure 10 **a** and **b**. The results observed that the weight loss of both the pure AA7075 matrix and the AA7075 reinforced by different mass fractions of OS after 30 days in the 0.1M **H_2SO_4** solution was less than 18 mg. Weight loss was also observed to be insignificant between 20 and 30 days. On the other hand, the corrosion rate of both the unreinforced AA7075 matrix and the AA7075 reinforced with different mass fractions of OS after 30 days in the 0.1M **H_2SO_4** solution was less than 9 mm / year. In addition, fig 10 **b** shows that the corrosion rate for all the samples was only significant during the first 5 days of immersion in 0.1MH_2SO_4 solution, after which it dropped significantly. Also, it can be observed from figures 10 **a** and **b** that the AA7075 reinforced with 15% OS had a higher corrosion resistance than the other samples. The introduction and regular distribution of OS particles inside the AA7075 alloy improved corrosion resistance, as evidenced by a decrease in mass loss and corrosion rate for all composites when immersed in both NaOH and H_2SO_4 solutions. Both B.M.Sathish and M. Sravanthi found similar observations in AA 7075 composites, reporting that corrosion resistance improves by increasing reinforcement [33, 34].

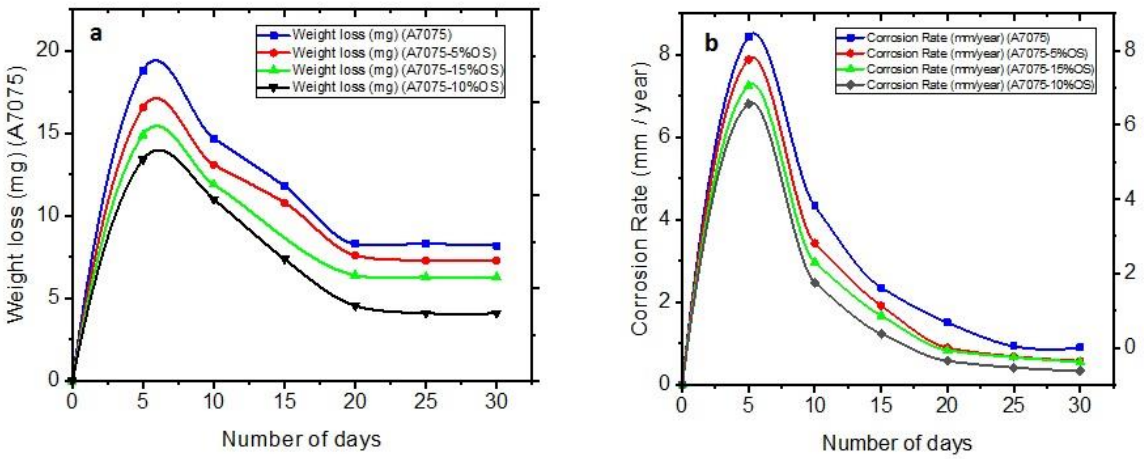

Fig 10 (a, b). Mass loss and corrosion rate of pure AA7075 and composites immersed in 0.1MH_2SO_4 solution.

SUMMARY AND CONCLUSIONS

The stir casting technique was used successfully to introduce Oyster shell particles into an AA7075 alloy. The results indicate that the waste OS powder can potentially be a good filler in the fabrication of AA7075 composites. The microstructure study reveals OS particle homogeneity dispersion within the AA7075 alloy. The influence of various mass fractions of OS particles on the mechanical characteristics of the AA 7075 alloy was examined, and the following data was recorded.

1. The hardness was increased from 37%, 61% and 88.7% for AA7075 reinforced with 5, 10 and 15% OS composite compared with unrienforced AA7075.
2. The yield strength was improved from 22.7%, 38.6% and 54.4% for AA7075 reinforced with 5, 10 and 15% OS composite compared with unreinforced AA7075. On the other hand, the ultimate compressive strength was improved from 10.7%, 19.8% and 25.9% for AA7075 reinforced with 5, 10 and 15% OS composite compared with unreinforced AA7075.
3. In addition, impact energy was declined from 15 (J) for pure AA7075 alloy to 8.1 (J) for AA7075/ 15 % OS.
4. The results revealed that the rate of corrosion and mass loss were decreased with increasing of mass fraction up to 15%.
5. The corrosion rate of both the unreinforced AA7075 matrix and the AA7075 reinforced by different mass fractions of OS after 30 days in the 0.1M NaOH and 0.1MH_2SO_4 solution was less than 2 and 9 mm / year, respectively.
6. Finally, the rate of corrosion and mass loss were lower in 0.1M NaOH solution when compared to 0.1M H_2SO_4 solution.

REFERENCES

[1] Mekonnen A.F and Mahmut A.S. Materials Used in Automotive Manufacture and Material Selection Using Ashby Charts // International Journal of Materials Engineering, 2018. Vol. 8, No 3. P. 40-54.

[2] Shin J.H, Choi H.J and Bae D.H. The structure and properties of 2024 aluminum composites reinforced with TiO2 nanoparticles // Journal of Mater. Sci. Eng. A, 2014. Vol. 607. P. 605–610.

[3] Torralba J, da Costa C and Velasco F. P/M aluminum matrix composites: An overview // Journal of . Mater. Process. Technol, 2003. Vol. 133. P. 203–206.

[4] Babalola P, Inegbenegbor A and Bolu C. The Development of Molecular Based Materials for Electrical and Electronic Applications // Journal of The Minerals, Metals and Materials Society, 2015. Vol. 67, No 4. P. 830-833.

[5] K. Ansar A and Jaber A.O. A Review on AA 6061 Metal Matrix Composites Produced by Stir Casting // Journal of Materials (Basel), 2021. Vol. 14, No 1. P. 175.

[6] Saravanan C, Subramanian K, Krishnan V.A and Narayanan R.S. Effect of Particulate Reinforced Aluminum Metal Matrix Composite –A Review // Journal of Mechanics and Mechanical Engineering, 2015. Vol.19, No 1. P. 23-30.

[7] Young R. Mineral Supplements, Copper, Nickel, and Cobalt Content of Oyster Shells // Journal of Agricultural and Food Chemistry. 1960. Vol. 8. P. 485-486.

[8] Chen Y, Lin S. Analysis of components in OS draconis and oyster shells // Journal of Fujian. Medical College. 1999. Vol. 33. P. 432-434.

[9] Lloyd D. Particle reinforced aluminum and magnesium matrix composites // Journal of Int. Mater. Rev. 1994. Vol. 39. P. 1–23.

[10] Padmavathi C, Upadhyaya A. Densification, microstructure and properties of super solidus liquid phase sintered 6711Al-SiC metal matrix composites // Journal of Sci. Sinter. 2010. Vol. 42. P. 363–382.

[11] Dinaharan I, Murugan N. Dry sliding wear behavior of AA6061/ZrB2 in-situ composite // Journal of Trans. Nonferrous Met. Soc. 2012. Vol. 22. P. 810–818.

[12] Laha T, Agarwal A, McKechnie T and Seal S. Synthesis and characterization of plasma spray formed carbon nanotube reinforced aluminum composite // Journal of Mater. Sci. Eng. A, 2004. Vol. 381. P. 249–258.

[13] Suthar J and Patel K. Processing issues, machining, and applications of aluminum metal matrix composites // Journal of Mater Manuf Process, 2018. Vol. 33. P. 499–527.

[14] Ramanathan A, Krishnan P.K and Muraliraja R. "A review on the production of metal matrix composites through stir casting–furnace design, properties, challenges, and research opportunities // Journal of Manuf Process, 2019. Vol. 42. P. 213–245.

[15] Alagarsamy S and Ravichandran M. Synthesis, microstructure and properties of TiO2 reinforced AA7075 matrix composites via stir casting route // Journal of Mater Res Exp, 2019. Vol. 6. P 1-27.

[16] Suresh S, Gowd G.H and Kumar M.D. Mechanical properties of AA 7075/Al 2 O 3/SiC nano-metal matrix composites by stir-casting method // Journal of Inst Eng (India): Series D, 2019. Vol. 100. P. 43–53.

[17] Nallusamy M, Sundaram S and Kalaiselvan K. Fabrication, characterization and analysis of improvements in mechanical properties of AA7075/ZrB2 in-situ composites // Journal of Measurement, 2019. Vol. 136. P. 356–366.

[18] Bhushan R K. Effect of SiC particle size and weight% on mechanical properties of AA7075 SiC composite // Journal of Adv Compos Hyb Mater, 2021. Vol. 4. P. 74–85.

[19] Manohar G, Pandey K and Maity S. Effect of sintering mechanisms on mechanical properties of AA7075/B4C composite fabricated by powder metallurgy techniques // Journal of Ceram Int, 2021. Vol. 47. P. 15147–15154.

[20] Singla D and Mediratta S R. Evaluation of Mechanical Properties of Al7075-Fly Ash Composite Material // Journal of Innov. Res. Sci. Eng. Technol, 2013. Vol. 2. P. 951–959.
[21] Dwivedi S P, Sharma S and Mishra R K. Effects of waste eggshells and SiC addition in the synthesis of aluminum hybrid green metal matrix composite // Journal of Green Process Synth,2017. Vol. 6. P. 113–123.
[22] Vivudh G, Balbir S and Mishra R K. Microstructural and mechanical characterization of novel AA7075 composites reinforced with rice husk ash and carbonized eggshells // Journal of Materials: Design and Applications.0(0), 2021. P. 1-15.
[23] Benjamin R E, Idongesit F E and Linus O A. Feasibility of Using Sea Shells Ash as Admixtures for Concrete // Journal of Environmental Science and Engineering. 2012, A 1 121-127 Formerly part of Journal of Environmental Science and Engineering, ISSN 1934-8932.
[24] Poovazhagan1 L, Rajkumar K and et al. Effect of Magnesium Addition on Processing the Al-0.8 Mg-0.7 Si/SiCp Metal Matrix Composites // Journal of Applied Mechanics and Materials. 2015. Vol. 787. P. 553-557.
[25] Suresh G, Selvaraj N, Kanmani S, Surya P and Rao C. Enhanced mechanical properties of AA6061-B_4C composites developed by a novel ultra-sonic assisted stir casting // Journal of Engineering Science and Technology, an International Journal, 2020. Vol. 23, No 5. P. 1233-1243.
[26] Praveen K S and Shantharaja M. Corrosion Behaviour of High-Strength Al 7005 Alloy and Its Composites Reinforced with Industrial Waste-Based Fly Ash and Glass Fiber: Comparison of Stir Cast and Extrusion Conditions // Journal of Materials, 2021. Vol. 14. P. 3929.
[27] Celebi Efe G, Yener T, Altinsoy I, Ipek M, Zeytin S, Bindal C. The effect of sintering temperature on some properties of Cu–SiC composite // Journal of Alloys and Compounds, 2011. Vol. 509. P. 6036–6042.
[28] Koppad P G, K. Kashyap K T, Shrathinth V, Shetty T A and R.G. R G. Microstructure and microhardness of carbon nanotube reinforced copper nanocomposites // Journal of Mater. Sci. Technol, 2013. Vol. 29. P. 605-609.
[29] Koti V, George R, A amd Murthy K V S. Mechanical properties of copper nanocomposites reinforced with uncoated and nickel coated carbon nanotubes // Journal of FME Transactions,2018. Vol. 46. P. 623-630..
[30] Venkatesh L, Arjunan T and Ravikumar K. Microstructural characteristics and mechanical behavior of aluminum hybrid composites reinforced with groundnut shell ash and B 4 C // Journal of Braz Soc Mech Sci Eng, 2019. Vol. 41. P. 295.
[31] Atuanya C, Esione A and Anene F. Effects of bamboo leaf stem ash on the microstructure and properties of cast Al–Si–Mg/bamboo leaf stem ash particulates composites // Journal of Chin Adv Mater Soc, 2018. Vol. 6. P. 543–552.
[32] Akbarpour M R, Salahi E, Alikhani F, Simchi A, Kim H S. Fabrication, characterization and mechanical properties of SiC nanoparticles and carbon nanotube reinforced copper based hybrid composites // Journal of Material Science & Engineering: A, 2013. Vol. 572. P. 83–90.
[33] Satish B M et.al. Effect of short glass fibres on the mechanical properties of cast ZA-27 alloy composites // Journal of Material and Design, 1996. Vol. 17, No, (5/6). P. 245-250.
[34] Sravanthi M, et al. Corrosion Studies on Aluminium-7075 Alloy and its Composites by Weight Loss Method // International Journal of innovative research & development, 2016. Vol. 5, No11. P. 23-27.